*Геология и геофизика*, *т. 65, № 8, с. 1184—1195*, DOI: 10.15372/GiG2023212, EDN: ABULYP
*Поступила в редакцию 27.04.2023, принята в печать 07.12.2023* *Опубликована онлайн: 10.12.2023*

УДК 550.832

# МУЛЬТИМИНЕРАЛЬНОЕ МОДЕЛИРОВАНИЕ И ОЦЕНКА ИНДЕКСА ХРУПКОСТИ МИНЕРАЛОВ С ИСПОЛЬЗОВАНИЕМ РЕЗУЛЬТАТОВ ИЗУЧЕНИЯ КЕРНА И ДАННЫХ ГИС В СКВАЖИНАХ НА УГОЛЬНОМ МЕСТОРОЖДЕНИИ ВОСТОЧНЫЙ БОКАРО (*Индия*)

**А. Банерджи**

*Department of Subsurface Team, Oil and Natural Gas Corporation Limited,*
*Bokaro, Jharkhand, 827001, India*

Точная оценка содержания и индекса хрупкости минералов имеет важное значение для разработки эффективных методов гидроразрыва угольных пластов, необходимого на угольном месторождении Восточный Бокаро в Индии. В настоящем исследовании объединены данные изучения керна бокового ствола и данные ГИС в скважинах. Основное внимание уделено скважине А-1, где был проведен рентгеноструктурный анализ керна бокового ствола для определения содержания минералов. Полученные минералогические данные были экстраполированы на скважину А-2 путем комбинирования результатов ГИС, рентгеноструктурного анализа и предыдущих исследований. Уравнения линейной регрессии, включающие известные минералы и данные ГИС в качестве входных параметров, использовались для расчета объемного содержания минералов в пластах. Надежность модели была подтверждена путем оценки минимальной разницы между прогнозируемыми и полученными логарифмическими кривыми. Индекс хрупкости определялся как геомеханическими методами, основанными на скорости продольных волн, так и минералогическими методами с учетом содержания кварца, полевого шпата и доломита. Сравнительный анализ значений индекса хрупкости продемонстрировал устойчивую тенденцию их изменения и их зависимость от содержания минералов. Данное исследование позволяет построить непрерывную мультиминеральную модель для случаев, когда данные по керну отсутствуют, а также дает представление о вариациях содержания минералов. Кроме того, корреляция между изменениями значений индекса хрупкости и содержанием минералов позволяет получить дополнительные сведения о геомеханических свойствах, необходимых для проектирования гидроразрыва угольных пластов. Представленные здесь результаты дают ценную информацию для оптимизации технологии гидроразрыва пласта на угольном месторождении Восточный Бокаро и служат основой для дальнейших исследований в аналогичных геологических обстановках.

*Мультиминеральная модель, геомеханический индекс хрупкости, минералогический индекс хрупкости*

# MULTIMINERAL MODELING AND BRITTLENESS INDEX ESTIMATION USING CORE AND GEOPHYSICAL WELL LOG DATA IN THE EAST BOKARO COALFIELD OF INDIA

**A. Banerjee**

Accurate assessment of mineral content and the brittleness index (*BI*) is crucial for designing effective hydraulic fracturing treatments in coal seams, a parameter required in the East Bokaro Coalfield in India. This study combines sidewall-core and well log data, focusing on well A-1, where X-ray diffraction analysis of sidewall cores was conducted to identify mineral content. The obtained mineralogical data were extrapolated to well A-2 through a synthesis of well log parameters, X-ray diffraction analysis, and prior research results. Linear regression equations incorporating known minerals and well log data as input parameters were employed to calculate volumetric mineral content in the formations. The reliability of the model was validated by assessing the minimal difference between predicted and observed log curves. Furthermore, the brittleness index was determined using both geomechanical methods based on compressional wave velocity and mineralogical methods incorporating quartz, feldspar, and dolomite content. Comparative analysis of *BI* values demonstrated a consistent trend, while variations in the mineralogic *BI* were observed in relation to mineral content. This study not only establishes a continuous multimineral model for cases with unavailable core data but also contributes to advancing the understanding of mineral content variations. Additionally, the correlation between *BI* variations and mineral contents enhances our knowledge of the geomechanical properties essential for design of hydraulic fracturing in coal formations. The results presented herein offer valuable insights for optimizing hydraulic fracturing strategies in the East Bokaro Coalfield and provide a foundation for further research in similar geologic settings.

*Multimineral model, geomechanical brittleness index, mineralogic brittleness index*

**© Банерджи А., 2024**
✉e-mail: Banerjee_Abir@ongc.co.in

## INTRODUCTION

Minerals form in the surface and subsurface rock owing to volcanic eruption, transportation of rock, pressure, and temperature in the formation. That is why the mineral composition in sedimentary, metamorphic, and igneous rock is different. Analysis of minerals in rock formations is important in understanding the depositional processes occurring in the Earth's system. The estimation of minerals using conventional well logs is difficult and less accurate. There are few cross-plotting techniques using well logs, such as neutron-density-sonic plots, and matrix identification plots separately cannot identify the minerals correctly in the formation (Clavier and Rust, 1976). For accurate identification, direct methods of X-ray diffraction (XRD) mineralogical tests are executed in core samples. However, the feasibility of extracting the core and its mineralogical analysis in every well is a constraint. Besides, continuous core extraction requires more time and involves more cost, so that it becomes challenging to extract continuous core. Therefore, an alternative method is used to determine the volume of multiminerals in a lithologic formation using conventional well logs and prior information on the minerals present in the area. The multimineral model visualizes the variation of mineral content in the subsurface formation. The mineral content can also provide a quantitative output of the brittleness in the formation which is expressed by an index known as the brittleness index (*BI*). The geomechanical and the mineralogical methods are two commonly used methods for estimating the *BI*. Although there is no accurate method for estimating the *BI*, the geomechanical and multimineral method acts as a guiding technique for estimating the *BI* without core sample analysis (Wang et al., 2015; Zhang et al., 2016).

The East Bokaro Coalfield is located in the Jharkhand state of the eastern part of India. The Bokaro Coalfield exhibits a complete succession of Gondwana sediments from the Basement to the Mahadeva Formation. The sequence is Basement, Talchir, Barakar, Barren, Raniganj, Mahadeva, and unconformity (Banerjee et al., 2023). For example, the Barakar formation is significant for the coalbed methane (CBM) reservoir development, as it contains all the coal seams inclusive of shale and sandstone. Generally, the lithology of the Bokaro Coalfield is categorized into coal, shale, and sandstone. In literature on the Bokaro Coalfield, a mineralogical study is conducted using XRD analysis, which shows that quartz and kaolinite are dominant while illite, montmorillonite, siderite, and analcime are intermediate minerals. Also, pyrite, dolomite, and calcite are observed in minor quantities in coal (Equeenuddin et al., 2016). Figure 1 represents the Bokaro Coalfield illustrating the surface exposure of various formations and the well location. The study area consists of two wells named A-1 and A-2 on the eastern side. In well A-1, a basic conventional well log suite including gamma-ray (GR), resistivity (MLR), density (ZDNC = ρ), photoelectric index (PE), and neutron porosity (NPHI = $\phi_n$) was recorded, and X-ray diffraction (XRD) analysis was carried out in ten sidewall core (SWC) samples to determine the

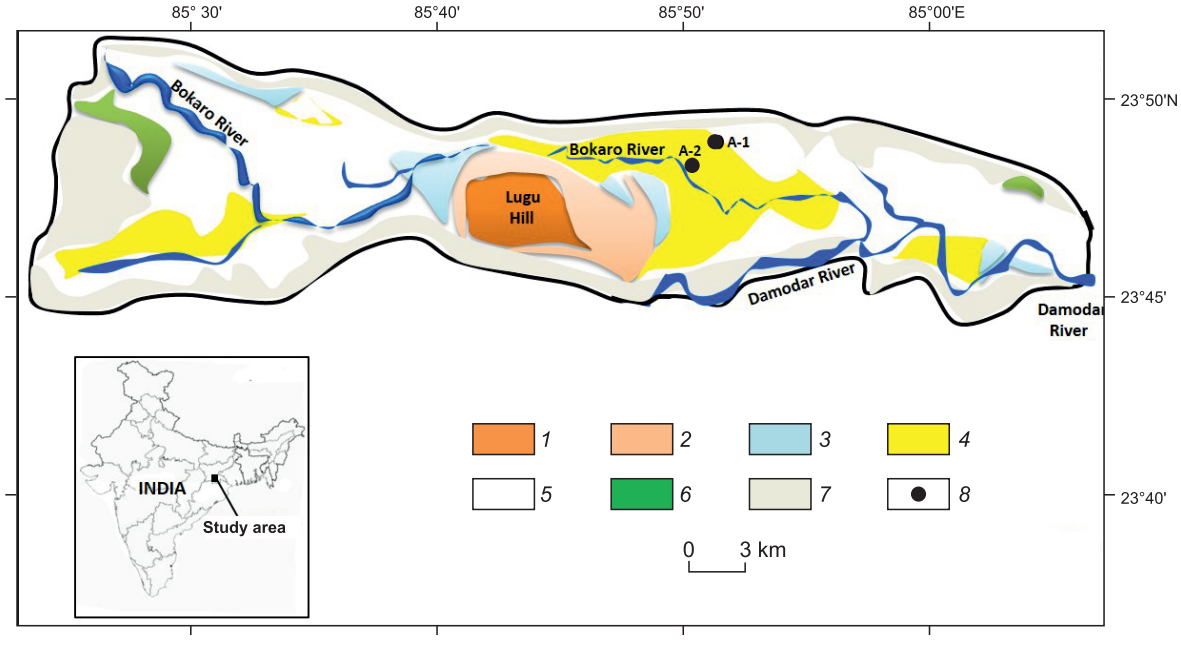


**Fig. 1. The geological map of the Bokaro Coalfield illustrates the surface exposure of different formations and two wells named A-1 and A-2 in the study area.**

*1* – Mahadeva, *2* – Panchet, *3* – Raniganj, *4* – Barren, *5* – Barakar, *6* – Talchir, *7* – Archaeans, *8* – well.

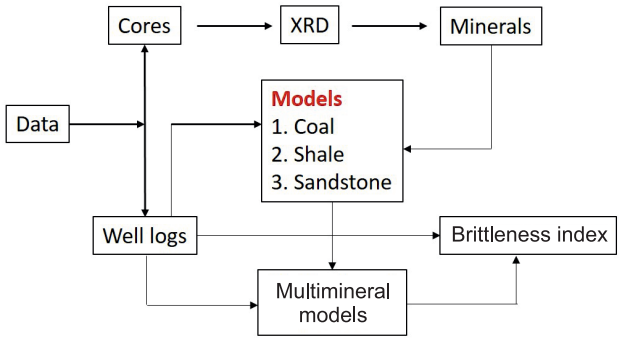


**Fig. 2. The adopted flowchart of the study in estimating the multimineral model and brittleness index along the well.**

mineral contents. In well A-2, compressional sonic slowness (SONIC = $\Delta t$) is an additional log available in the basic conventional well log suite.

The lack of understanding of mineral deposition and the absence of a standardized model has motivated us to undertake this study with the objectives (a) to determine the mineral contents from the XRD study of SWC samples in well A-1, (b) to generate multimineral models and volumetric estimation of minerals in well A-2 by solving linear equations using geophysical well logs and minerals as input parameter, and (c) to estimate the brittleness index of the formation using the geomechanical and mineralogical approach. A flowchart was adopted to attain the objectives. Figure 2 depicts the adopted flowchart, which illustrates core and well log as input data in establishing the models. The identified minerals from the XRD study of cores were incorporated with geophysical well logs to determine the percentage of minerals in the wellbore. The lithology, such as sandstone, shale, and coal, was distinguished based on well log parameters (Banerjee et al., 2023). In these zones, its mineral contents were classified, and based on mineralogic volume, the *BI* was estimated, and the same was compared with the geomechanical *BI* estimated using a sonic log.

## METHODS

***X*-ray diffraction (XRD) analysis.** The XRD analysis in the laboratory provides accurate mineral identification by interpreting the characteristics of peak positions either through eye estimation or by an automated computerized matching technique with the incident angle (Hillier, 2003). The presence of minerals from the peak intensity in the XRD curve uses a generalized instrument that is independent of the semiquantitative method (Fisher and Underwood, 1995; Gandhi et al., 2010). In this method, the percentage of the mineral present in a sample is calculated from the XRD peak heights ($i$) and standard intensity factors ($c$) of the composite minerals. The standardized equation is presented in the following equations:

$$m_i = \left( \frac{c_i i_i}{\sum_{n=1}^{m} c_n i_n} \right), \tag{1}$$

where $m_i$ denotes the abundance of the $i$th mineral; $i_i$ is the peak intensity of the $i$th mineral; $c_i$ is a constant intensity factor of mineral used to transform intensity into abundance; and $m$ is the number of minerals. Values of the intensity factor ($c_i$) of the identified mineral peaks were assigned as mentioned by Gandhi et al. (2010) for the determination of mineral abundance. In well A-1, ten SWC at different depths were crushed for XRD analysis (plot between intensity (counts per second) versus angle) to compute the mineral contents. In Table 1, the SWC sample number, depth of extraction, mineral content, and respective well log magnitude of well A-1

Table 1. **Mineral contents from XRD analysis and well log magnitude at respective depths**

| SWC sample No. | Depth, m | Minerals (XRD) | GR (API) | MLR (Ohm·m) | ZDNC (g/cm$^3$) | NPHI (v/v ) |
|---|---|---|---|---|---|---|
| SWC-01 | 674.0 | Illite, kaolinite, montmorillonite, mica, quartz | 125 | 600 | 2.15 | 0.30 |
| SWC-02 | 629.0 | Illite, kaolinite, montmorillonite, mica, quartz, feldspar | 170 | 250 | 2.54 | 0.30 |
| SWC-03 | 572.6 | Illite, kaolinite, mica, quartz, siderite | 175 | 150 | 2.68 | 0.24 |
| SWC-04 | 419.0 | Illite, mica, quartz, siderite, carbonaceous minerals | 190 | 100 | 2.38 | 0.30 |
| SWC-05 | 418.5 | Illite, montmorillonite, mica, quartz | 162 | 10 | 2.60 | 0.24 |
| SWC-06 | 418.0 | Feldspar, quartz, calcite, dolomite, siderite, and pyrite | 135 | 0.3 | 0.21 | 2.55 |
| SWC-07 | 417.5 | Illite, montmorillonite, mica, quartz, siderite | 167 | 10 | 0.27 | 2.55 |
| SWC-08 | 405.5 | Quartz, dolomite | 60 | 300 | 0.09 | 2.74 |
| SWC-09 | 404.5 | Illite, mica, dolomite, quartz | 67 | 200 | 0.10 | 2.70 |
| SWC-10 | 402.9 | Illite, kaolinite, mica, quartz, siderite | 110 | 80 | 0.18 | 2.53 |

are shown. The peaks on the intensity curves in the XRD pattern permit identifying illite, kaolinite, smectite, montmorillonite, siderite, quartz, feldspar, mica, and dolomite in the SWC sample. Figure 3*a–d* illustrates a few XRD patterns depicting the intensity (count per second) versus 2θ (degree) plot drawn on the SWC samples: (a) SWC-01 at 674.0 m, (b) SWC-02 at 629.0 m, (c) SWC-07 at 417.5 m, and (d) SWC-09 at 404.5 m. Also, the microscopy study of the SWC samples shows mineral contents. Figure 4*a–d* represents the study of sample SWC-02 under the microscope (a) at 629.0 m and (b) the enlarged view of sample SWC-02 shows mica, oxidized matter, and carbonaceous content, (c) similar study of sample SWC-09 at 404.5 m shows the presence of mica and quartz.

**Multimineral modeling.** The identification of minerals is difficult from the quick-look analysis of the conventional well logs, but the volumetric content of minerals can be modeled using geophysical logs provided that the number and the type of minerals are known. Hence, to estimate the mineral volume and content, the prior information on minerals in the formation is an input to solve the set of linear equations. Thus, multimineral modeling utilizes the relationship between the set of known and unknown parameters in the set of linear equations. Here, log measurements are known parameters, and the properties of the mineral constituents are the unknown parameters. The log measurements used in the models are gamma ray, conductivity ($C$ = 1/MLR), density (ρ), photoelectric parameter ($L$ = ρ.PE), compressional slowness (Δ$t$), and neutron porosity (NPHI = $\phi_n$). The proposed multimineral model uses seven equations to solve seven unknowns (six minerals and porosity). The first six equations can be written as

$$X = \phi X_f + \sum_{i=1}^{6} M_i X_i \,, \tag{2}$$

where $X$ represents the log magnitude; $\phi$ is the porosity obtained from multimineral modeling; $X_f$ represents the log magnitude in the fluid where subscript $f$ stands for fluid; $M_i$ represents the concentration of a respective min-

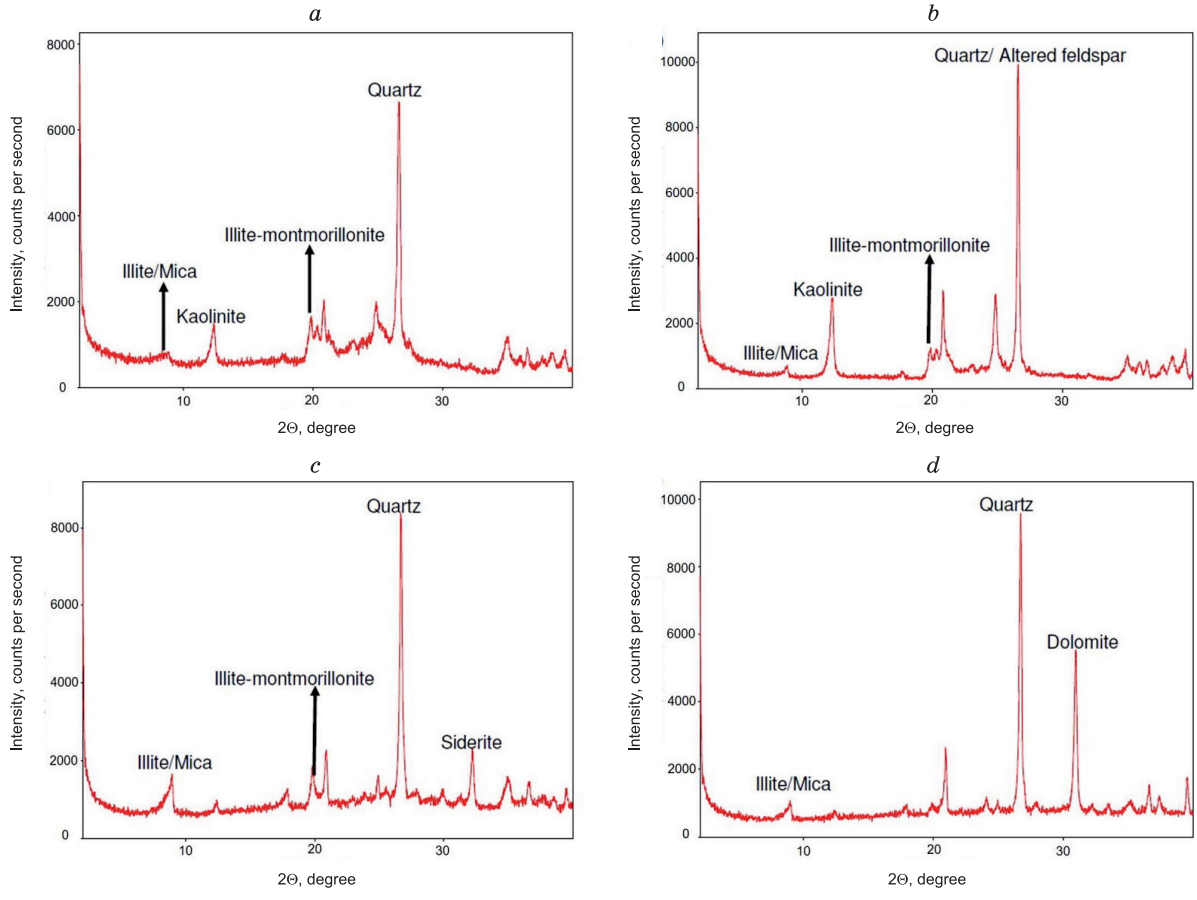


**Fig. 3. The XRD pattern depicting the intensity (count per second) versus 2θ (degree) plot conducted on the sidewall core (SWC) samples:**

*a* – SWC-01 at 674.0 m; the peak intensity detects illite/mica, kaolinite, montmorillonite, and quartz; *b* – SWC-02 at 629.0 m; peak intensity detects illite, kaolinite, montmorillonite, and quartz/feldspar; *c* – SWC-07 at 417.5 m, shows the additional presence of siderite mineral; and *d* – SWC-09 at 404.5 m, shows dolomite as additional content.

eral; and $X_i$ represents the log magnitude in the mineral formation, where the subscript ($i$ = 1 to 6) in $M_i$ and $X_i$ denotes the mineral concentration of six minerals. Equation (2) generates six separate equations for the different log values, such as (1) GR, (2) ρ, (3) $\phi_n$, (4) $L$, (5) $\Delta t$, and (6) $C$. Thus, using the log values in equation (2), six linear equations can be established. The seventh equation is established considering the sum of the effective porosity and the mineral content equal to the total volume of the rock. Thus, the equation is expressed as

$$1 = \phi + \sum_{i=1}^{6} M_i \,, \tag{3}$$

where the notations are the same as described previously. Subsequently, solving the set of seven linear equations determines the seven unknown parameters. The equations are expressed in the matrix form as follows:

$$\begin{bmatrix} GR_f & GR_f & GR_f & GR_f & GR_f & GR_f & GR_f \\ \rho_f & \rho_f & \rho_f & \rho_f & \rho_f & \rho_f & \rho_f \\ \phi_{nf} & \phi_{nf} & \phi_{nf} & \phi_{nf} & \phi_{nf} & \phi_{nf} & \phi_{nf} \\ L_f & L_f & L_f & L_f & L_f & L_f & L_f \\ \Delta t_f & \Delta t_f & \Delta t_f & \Delta t_f & \Delta t_f & \Delta t_f & \Delta t_f \\ C_f & C_f & C_f & C_f & C_f & C_f & C_f \\ 1 & 1 & 1 & 1 & 1 & 1 & 1 \end{bmatrix} \begin{bmatrix} \phi \\ M_1 \\ M_2 \\ M_3 \\ M_4 \\ M_5 \\ M_6 \end{bmatrix} = \begin{bmatrix} GR \\ \rho \\ \phi_n \\ L \\ \Delta t \\ C \\ 1 \end{bmatrix}, \tag{4}$$

The matrix system presented in equation (4) illustrates the simultaneous matrix inversion calculation performed for the mineral composition (Singh et al., 2013) which can be expressed as

$$FM = W \,, \tag{5}$$

where $F$ is the matrix of the physical properties of rock constituents; $M$ is the matrix of the mineral constituents; and $W$ is the measured well log values. The dominant rock constituents that were applied in matrix $F$ are listed in Table 2. The mineral volume can be estimated by solving an inverse problem in equation (5):

$$M = F^{-1}W \,. \tag{6}$$

Thus, by solving equation (6), the quantification of minerals can be executed. Banerjee and Chatterjee (2022) discussed well log cutoff parameters in the Bokaro Coalfield to distinguish sandstone, shale, and coal, based on this zonations were prepared in well A-2. Table 2 shows the mineral contents and well log parameters

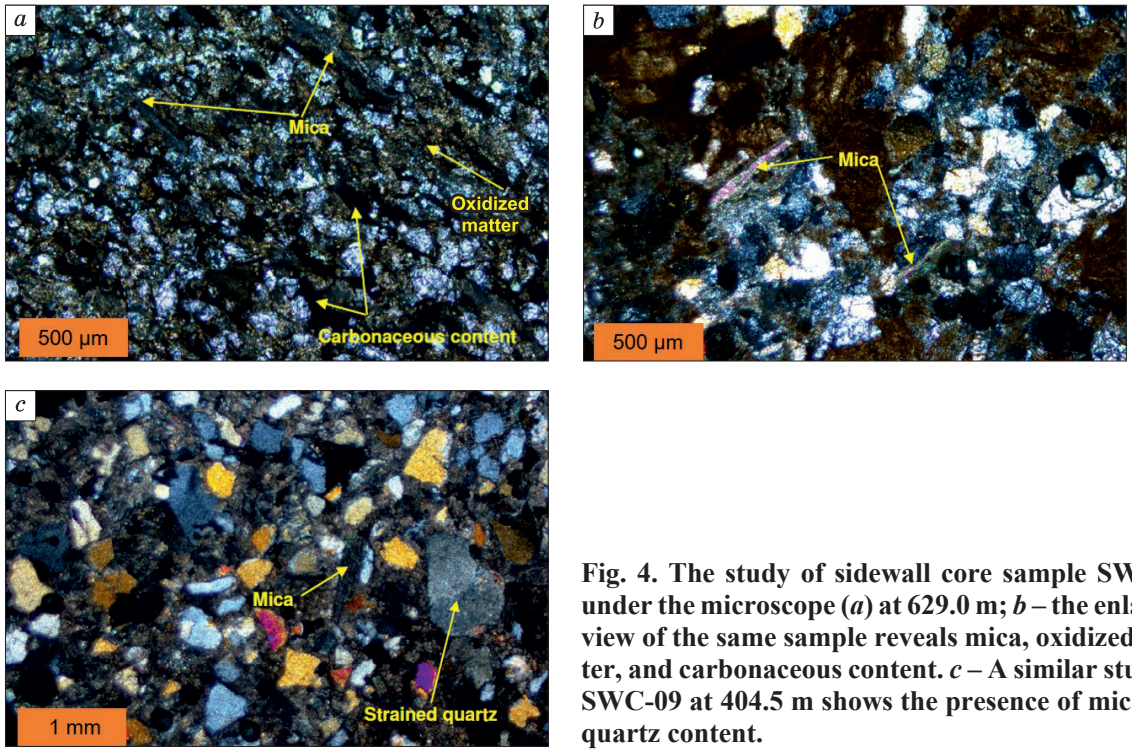


**Fig. 4. The study of sidewall core sample SWC-02 under the microscope (*a*) at 629.0 m; *b* – the enlarged view of the same sample reveals mica, oxidized matter, and carbonaceous content. *c* – A similar study of SWC-09 at 404.5 m shows the presence of mica and quartz content.**

Table 2. **The mineral contents and well log parameters used in the shale, sandstone, and coal during processing**

| Models | Minerals | Density | NPHI | DTC | U | GR |
|---|---|---|---|---|---|---|
| Shale | Illite | 2.78 | 0.300 | 70 | 6.7 | 190 |
| | Kaolinite | 2.62 | 0.300 | 70 | 6.5 | 180 |
| | Smectite | 2.63 | 0.210 | 85 | 7.6 | 150 |
| | Quartz | 2.65 | 0.090 | 50 | 5.0 | 90 |
| | Feldspar | 2.67 | 0.090 | 53 | 8.7 | 130 |
| | Dolomite | 2.84 | 0.025 | 43 | 9.6 | 50 |
| Sandstone | Illite | 2.78 | 0.080 | 70 | 3.1 | 65 |
| | Kaolinite | 2.62 | 0.450 | 85 | 5.3 | 104 |
| | Smectite | 2.63 | 0.210 | 85 | 7.6 | 168 |
| | Quartz | 2.55 | 0.070 | 70 | 5.0 | 85 |
| | Feldspar | 2.60 | 0.060 | 53 | 8.7 | 165 |
| | Dolomite | 2.84 | 0.025 | 43 | 9.6 | 30 |
| Coal | Coal | 1.27 | 0.600 | 132 | 0.9 | 70 |
| | Illite | 2.78 | 0.010 | 85 | 7.1 | 170 |
| | Kaolinite | 2.62 | 0.010 | 85 | 5.5 | 180 |
| | Smectite | 1.80 | 0.210 | 120 | 0.4 | 80 |
| | Quartz | 2.65 | 0.050 | 50 | 5.0 | 15 |

Note. In shale and sandstone, illite, kaolinite, smectite, quartz, dolomite, orthoclase, and siderite were selected. Coal is considered a special mineral with the inclusion of illite, kaolinite, smectite, and quartz.

used during the processing of the shale, sandstone, and coal lithology. In shale and sandstone, minerals, such as illite, kaolinite, smectite, quartz, dolomite, orthoclase, and siderite, were selected. Coal is considered a special mineral along with the inclusion of illite, kaolinite, smectite, and quartz. Solving the matrix equation (4) gives the effective porosity, while the total porosity is calculated for comparing the effective porosity with the total porosity. The total porosity ($\phi_T$) is calculated using the following equation:

$$\phi_T = \frac{\rho_{ma} - \rho_b}{\rho_{ma} - \rho_f}, \tag{7}$$

where $\rho_{ma}$ is the matrix density; $\rho_b$ is the bulk density obtained from the density log; and $\rho_f$ is the fluid density (1.0 g/cm$^3$). Figure 5 represents the layout illustrating (1) the color code of lithologic formations in the first track, such as illite, kaolinite, montmorillonite, quartz, dolomite, feldspar, siderite, and coal; (2) the volume of minerals (fraction) in the second track; (3) depth (m) in the third track; (4) variation in total and effective porosity in the fourth track; (5) the fifth to ninth tracks validate the results from the correlation between actual and predicted log curve of NPHI, GR, ZDNC, PEF, and SONIC.

**Brittleness index estimation.** The estimation of the *BI* using well log data is a preferred method, as it involves low cost and provides continuity throughout the well. Both the geomechanical and mineralogical methods can be used to estimate the *BI*. Previous studies by Jarvie et al. (2007) and Jin et al. (2015) show that the brittleness estimated from the mineralogical method is more reliable compared to that estimated by the geomechanical approach for a shale reservoir. The geomechanical approach relates the *BI* in terms of Young's modulus and Poisson's ratio empirically using sonic velocity, which is further implemented to estimate the *BI* (Mallick, 1995; Lai et al., 2015). The empirical equations for the estimation of geomechanical parameters and the *BI* are as follows:

$$Y = \rho V_s^2 \left( \frac{3V_p^2 - 4V_s^2}{V_p^2 - V_s^2} \right), \tag{8}$$

$$\nu = \frac{V_p^2 - 2V_s^2}{2(V_p^2 - V_s^2)}, \tag{9}$$

$$BI_Y = \frac{Y - Y_{\min}}{Y_{\max} - Y_{\min}}, \quad BI_\nu = \frac{\nu - \nu_{\max}}{\nu_{\min} - \nu_{\max}},$$

$$BI_g = \frac{BI_Y - BI_\nu}{2}, \tag{10}$$

where $Y$ is Young's modulus; ν is Poisson's ratio; $BI_Y$ and $BI_\nu$ are the brittleness indices obtained from $Y$ and ν, respectively. $BI_g$ is the average magnitude of the geomechanical *BI*. The notation 'min' and 'max' denote the

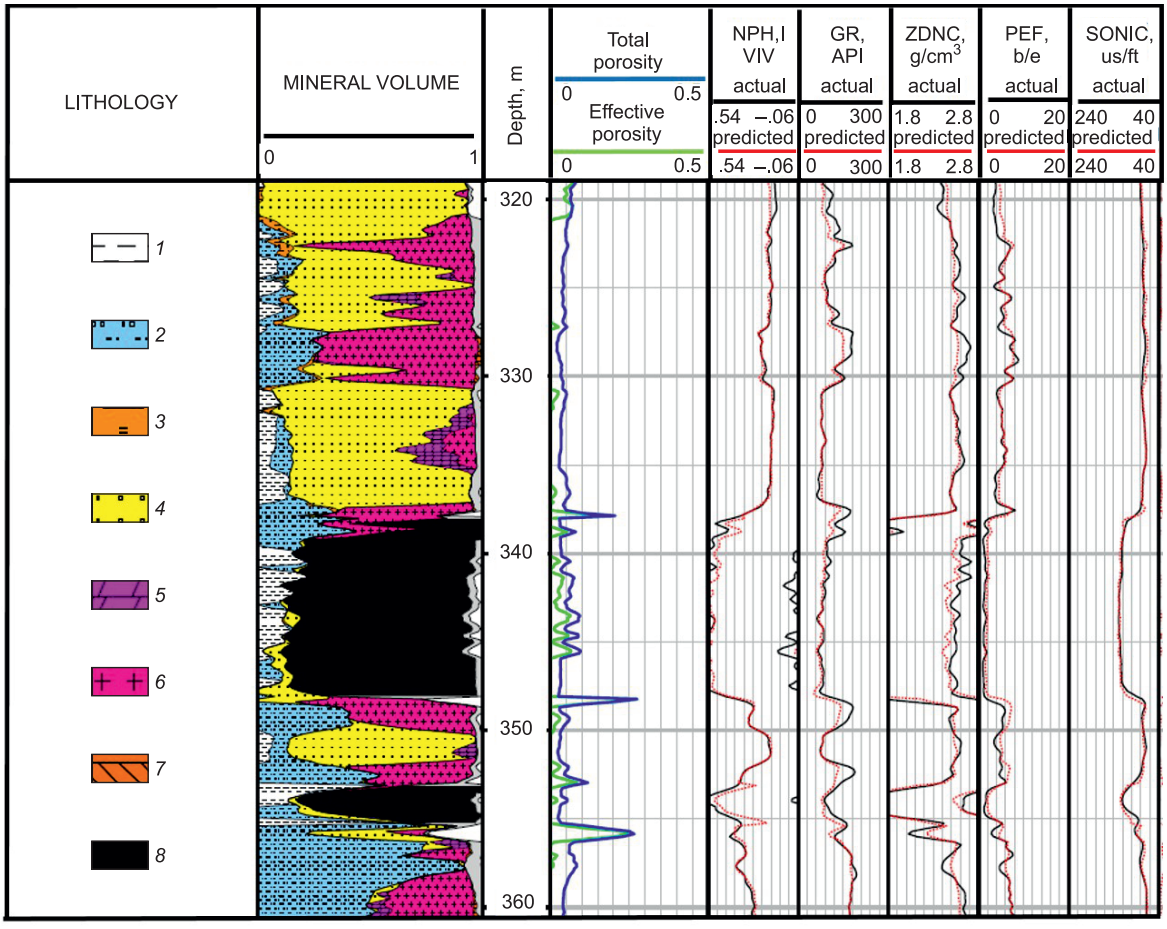


**Fig. 5. The layout represents (1) the color code of lithologic formations, such as:**

illite (*1*), kaolinite (*2*), montmorillonite (*3*), quartz (*4*), dolomite (*5*), feldspar (*6*), siderite (*7*), and coal (*8*) in the first track; (2) the volume of minerals (fraction) in the second track; (3) depth (m) in the third track; (4) variation in total and effective porosity in the fourth track; and (5) the fifth to ninth tracks validate the results from the correlation between actual and predicted log curve of NPHI, GR, ZDNC, PEF, and SONIC.

minimum and maximum values, respectively. In the mineralogical approach, the volume of mineral content estimates the *BI* using established equations. Jarvie et al. (2007) proposed the *BI* as the ratio of the volume of quartz content to the total volume of the minerals contained in the rock formation. However, Wang and Gale (2009) modified the equation using the sum of the volume of quartz and dolomite divided by the total volume of mineral content. Later, Jin et al. (2015) considered the sum of the volume of quartz, feldspar, mica, and carbonate minerals divided by the total volume of minerals in the rock formation. The previously used mineralogical approach for the *BI* estimation is listed in Table 3. In our case, quartz, feldspar, and dolomite were present in the formation, and based on the methods presented in Table 3, the mineralogic *BI* is obtained by integrating the tabulated equation. The equation is expressed as

$$BI = \frac{V_q + V_F + V_d}{V_T}, \qquad (11)$$

where $V$ represents the volume of minerals and the subscripts have the following meanings: $q$, quartz; $F$, feldspar; $d$, dolomite; and $T$, total volume of the

Table 3. **List of the equations considered in the previous study in different formations**

| Formula | Variable definition | References |
|---|---|---|
| $BI = \frac{V_q}{V_T}$ | $V_q$ is the volume of quartz; $V_T$ is the total volume of minerals. | Jarvie et al., 2007 |
| $BI = \frac{V_q + V_d}{V_T}$ | $V_q$ and $V_d$ are the volumes of quartz and dolomite. | Wang and Gale, 2009 |
| $BI = \frac{V_q + V_F + V_M + V_{carb}}{V_T}$ | $V$ is the volume of minerals: $q$ –quartz; $F$ – feldspar; $M$ – mica; *carb* – carbonate. | Jin et al., 2015 |
| $BI = \frac{V_q + V_{cal} + V_{al}}{V_q + V_{cal} + V_{al} + V_m + V_{cl}}$ | $V$ is the volume of minerals: $q$ – quartz; *cal* – calcite; *al* – albite; $m$ – muscovite; *cl* – clay. | Lai et al., 2015; Gholami et al., 2016 |

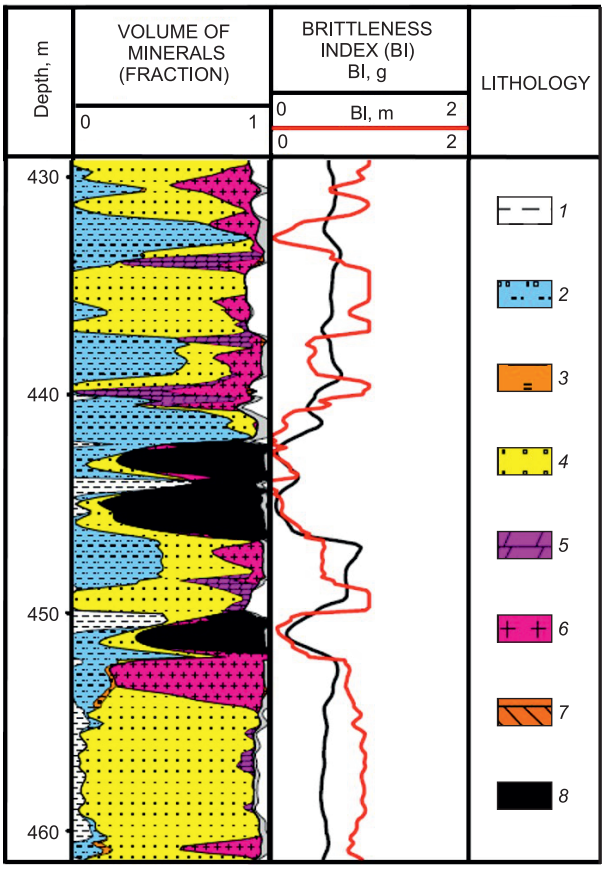


**Fig. 6. The layout representing the (1) depth (m) in the first track; (2) the volume of minerals (fraction) in the second track; (3) estimated geomechanical brittleness index BI (g) in a black line and mineralogic brittleness index BI (m) in a blue line; and (4) the fourth track represents the color code of illite, kaolinite, montmorillonite, quartz, dolomite, feldspar, siderite, and coal.**

minerals. The result from equation (13) is presented in Fig. 6, where the layout shows the (1) depth (m) in the first track; (2) volume of minerals (fraction) in the second track; (3) estimated geomechanical [*BI* (g)] in a black line and mineralogic [*BI* (m)] in a blue line; and (4) the fourth track represents the color code of lithologic formations, such as illite, kaolinite, montmorillonite, quartz, dolomite, feldspar, siderite, and coal. The *BI* estimated from both methods was cross-plotted. Figure 7 illustrates the cross-plot of the *BI* (geomechanical) versus *BI* (mineralogic) of (a) all formations where color dots in red, green, and blue are shale, sandstone, and coal, respectively, (b) shale formation only, (c) sandstone formation only, and (d) coal formation only. The cross-plots in Fig. 7*b* show scattered *BI* dots, and the *BI* in shale increases linearly up to 0.6, and then *BI* (geomechanical) follows a trend toward a constant value 0.6–0.7, while the *BI* (mineralogic) increases from 0.6 to 1.0. Also, in some shale formations, the *BI* (mineralogic) is estimated at a lower value compared to the *BI* (geomechanical). In Fig. 7*c*, the *BI*, both geomechanical and mineralogic, are concentrated toward the higher side in sandstone, and in Fig. 7*d*, the *BI* is concentrated toward the lower side in coal. The plot of the *BI* (mineralogic) versus the sum of the volume of quartz, feldspar, and dolomite [volume (Q + F + D)] is shown in Fig. 8. The plot of the *BI* (mineralogic) versus volume (Q + F + D) (a) for shale, sandstone, and coal, (b) for a shale formation, (c) for a sandstone formation, and (d) for a coal formation. Summarizing Figs. 7 and 8, Table 4 shows the average range of the *BI* (geomechanical), the *BI* (mineralogic) and [volume (Q + F + D)] in shale, sandstone, and coal, respectively.

## DISCUSSION

The use of the harmonic mean in equation (1) for XRD studies (specifically, in determining mineral content), is closely tied to the nature of crystalline materials and the analysis of their diffraction patterns. When analyzing XRD data in a laboratory setting to identify and quantify minerals in a sample, the harmonic mean is often incorporated to account for the anisotropic nature of crystallite size in polycrystalline materials. Geologic samples are typically polycrystalline; that is, they consist of many small randomly oriented crystalline domains. Each domain may have different crystallographic orientations and sizes. The harmonic mean is used to average the sizes of these crystalline domains along different crystallographic directions, providing a more representative measure of the overall crystallite size. Crystallites within a sample may exhibit different sizes along different crystallographic directions. This anisotropy is especially relevant in geologic materials in which crystal growth may occur preferentially in certain directions. The harmonic mean considers the reciprocal of the crystallite sizes

Table 4. **The *BI* computed from geomechanical and mineralogical analysis with the volume of quartz, feldspar, and dolomite in shale, sandstone and dolomite**

| Lithology | $BI_g$ (average) | $BI_m$ (average) | Volume (quartz + feldspar + dolomite) |
|---|---|---|---|
| Shale | 0.45–0.75 | 0.15–0.95 | 0.01–0.90 |
| Sandstone | 0.50–0.75 | 0.60–0.95 | 0.50–0.95 |
| Coal | 0.01–0.35 | 0.01–0.30 | 0.01–0.40 |

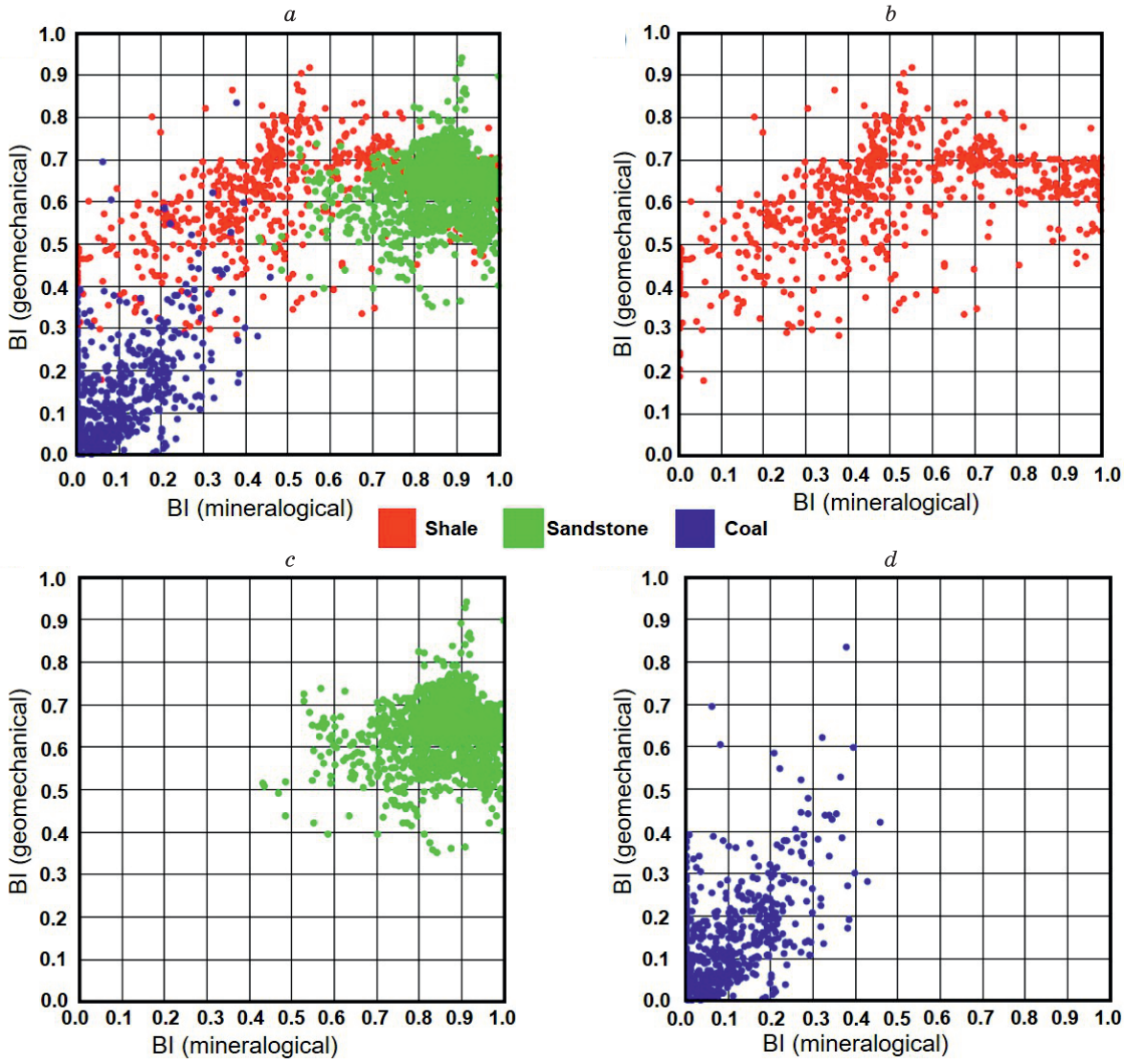


**Fig. 7. The geomechanical brittleness index [BI (geomechanical)] versus the mineralogic brittleness index [BI (mineralogical)] plot shows a scattered trend:**

*a* – brittleness plot shown for shale, sandstone, and coal; *b* – brittleness plot in the shale formation; *c* – brittleness plot in the sandstone formation; and *d* – brittleness plot in the coal formation.

along different directions, emphasizing the influence of smaller sizes in the overall average. Thus, the use of the harmonic-mean equation for mineral content determination enhances the accuracy of estimating the average crystallite size in polycrystalline materials. At the same time, the arithmetic mean approach in equation (2) for the determination of multimineral modeling from well log data is considered due to its simplicity, ease of interpretation, and computational efficiency, making it suitable for quick assessments and initial screening of mineral content in subsurface formations. The arithmetic mean is straightforward to calculate and computationally efficient. In well log analysis, in which large datasets are often involved, simplicity and speed are essential for quick and practical modeling. The arithmetic mean provides a single representative value that is easy to interpret. In the context of well log data, mineral content is often presented as an average percentage, simplifying the understanding of the overall mineral composition. Well log data are often measured at discrete depths along a borehole. The arithmetic mean is well-suited for summarizing data at these discrete points and is particularly useful when dealing with well log curves representing different minerals. The arithmetic mean also allows a rapid initial estimation without the need for more complex and time-consuming modeling techniques.

The concept of matrix degeneracy is related to linear algebra, and it typically refers to a matrix that is singular or nearly singular. A matrix is said to be degenerate if its determinant is zero or very close to zero,

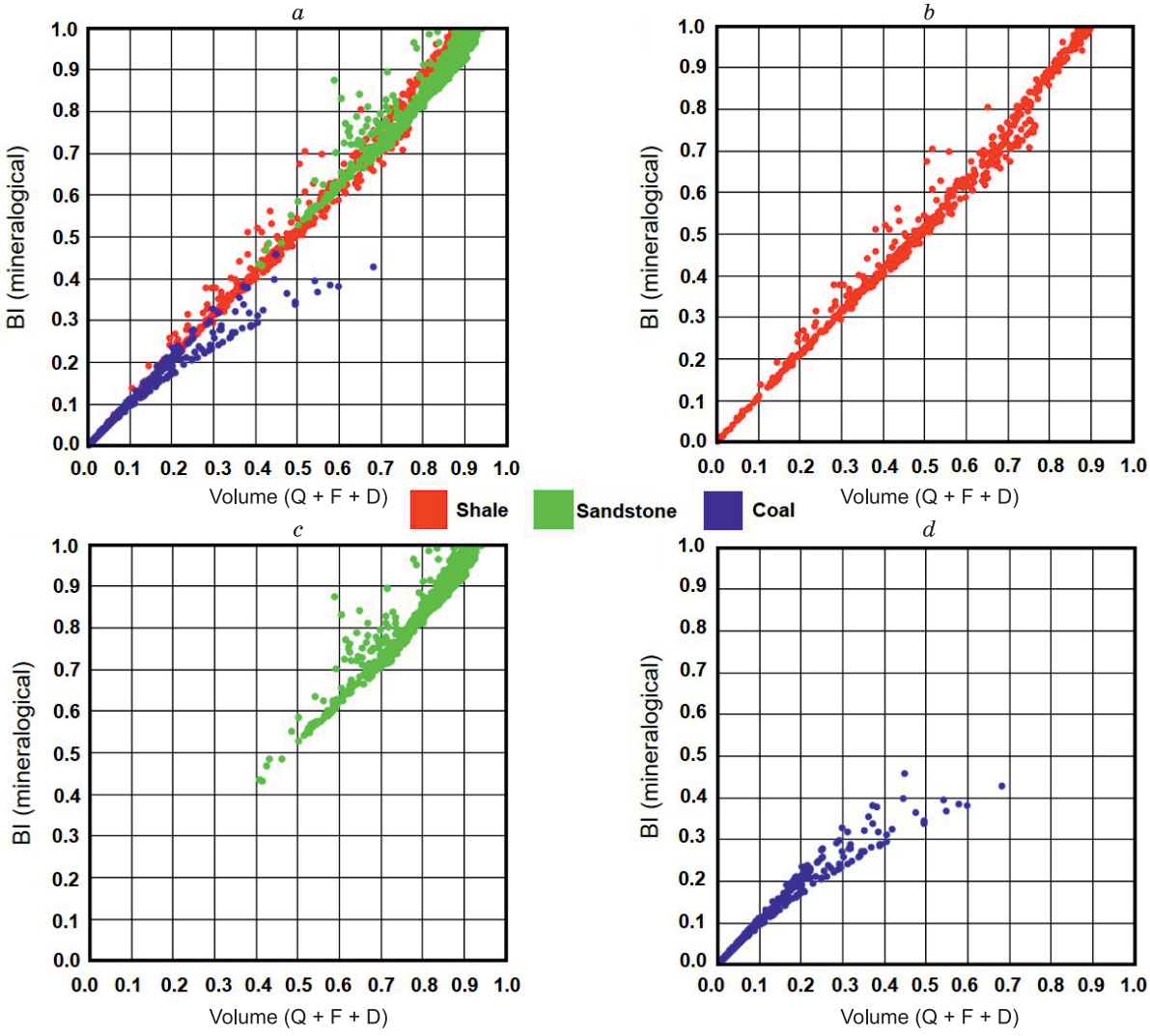


**Fig. 8. The mineralogic brittleness index [BI (mineralogical)] versus the sum of the volumes of quartz, feldspar, and dolomite [Volume (Q + F + D)] plot shows a linear trend:**

*a* – the plot represents shale, sandstone, and coal formations; *b* – the plot represents the shale formation; *c* – the plot represents the sandstone formation; *d* – the plot represents the coal formation.

which implies that the matrix is not invertible. Proving the nondegeneracy of a matrix in equations (5) and (6) is often crucial in various mathematical and computational contexts, including those dealing with multivariate analysis, optimization problems, and systems of linear equations. A nondegenerate matrix is more likely to have a unique solution, and its properties are generally better understood. Here, the determinant of a square matrix $F$ in equation (6) is denoted by $|F|$, which is nonzero, proving that the matrix is nondegenerate. Also, the rank of the matrix is equal to the size of the matrix, and $F$ is a positive definite symmetric matrix, which proves that it is nondegenerate.

The adopted methodology for generating a multimineral model within a well using available well logs and prior inputs of mineral contents in the formation has proven to be robust and accurate. The resulting model offers a comprehensive volumetric distribution of minerals along the wellbore, facilitating the estimation and standardization of percentagewise mineral distribution in the subsurface formation. The reliability of this multimineral model is underscored by the minimal difference observed between the observed and predicted log curves, affirming its accuracy. Furthermore, our investigation into brittle behavior, indicative of quartz, feldspar, and dolomite presence, reveals a linear increase in the brittleness index with the volume of these minerals. This result is consistent with those of previous studies that have shown a positive correlation between the *BI* and quartz content in shale formations (Jin et al., 2015; Zhang et al., 2016). The *BI* values obtained in this study

can be used to identify the most brittle zones in the coal seams, which are ideal targets for hydraulic fracturing treatments. The data in Table 4 show that the *BI* values are the highest in the sandstone formation, followed by those in the shale and coal formations. This suggests that the sandstone formation is the most brittle, which is consistent with results of previous studies that have shown that sandstone formations are more brittle than shale or coal formations (Zhang et al., 2016). The data in Table 4 also show that the volume (Q + F + D) values are the highest in the sandstone formation, followed by those in the shale and coal formations. This suggests that the sandstone formation has the highest porosity and permeability, which is consistent with previous studies that have shown that sandstone formations are more porous and permeable than shale or coal formations (Jin et al., 2015). Accurate assessment of mineral content and the brittleness index is crucial for designing effective hydraulic fracturing treatments in coal seams. Our methodology provides a reliable and efficient way of generating a multimineral model within a well, which can be used to estimate the volumetric distribution of minerals and identify the most brittle zones. This information can be used to optimize hydraulic fracturing treatments and improve production rates in the East Bokaro Coalfield. Further research is needed to extend our results to other coalfields.

## CONCLUSIONS

A comprehensive investigation of the CBM reservoir was conducted to address the critical need for accurate characterization of mineral content and the brittleness index. Utilizing known minerals and well log data as input parameters, volumetric mineral content in the formations was obtained. The reliability of our model was confirmed by the minimal difference observed between predicted and observed log curves. The correlation established between *BI* variations and mineral contents enhances our ability to predict and optimize hydraulic fracturing treatments in coal formations. A comparative analysis of *BI* values revealed a consistent trend, though the mineralogic *BI* exhibited variability concerning mineral content. These insights contribute to the broader field of reservoir engineering and underscore the importance of integrating multiple methods for a comprehensive understanding of subsurface formations.

## ACKNOLEDGMENTS AND FUNDING

The author is thankful to Oil and Natural Gas Corporation Limited, India, for the support to conduct the work. The author is also grateful to Mr. A.K. Dwivedi, (Ex-Director (E)), Mr. N.C. Pandey, (Ex-Director (T&FS)), Mr. Aditya Johri (ED-AM, Bokaro), Mr. Aloke Das (CGM-Reservoir), Mr. Pradipta Mitra (GM-Reservoir), and Nawin Lugun (GM-Geology) of Oil and Natural Gas Corporation Limited for the support in this study. The author acknowledges the support of Mr. Shubham Dimri (Support Executive) for using the Geolog software (Emerson Paradigm). No funding was received in the preparation of this manuscript.

## DATA AVAILABILITY STATEMENT

The data that support the results of this study are available with the CBM, Bokaro Asset of Oil and Natural Gas Corporation Limited, India.

## REFERENCES

**Banerjee, A., Chatterjee, R.,** 2022. Fracture analysis using Stoneley waves in a coalbed methane reservoir. Near Surf. Geophys. 20, 710–722, doi: 10.1002/nsg.12176.

**Banerjee, A., Chatterjee, R., Singha, D.K.,** 2023. Anisotropy and fracture analysis for coalbed methane reservoir development in Bokaro coalfield, India. Geophys. Prospect. 71, 1914–1932, doi: 10.1111/1365-2478.13236.

**Clavier, C., Rust, D.H.,** 1976. MID plot: A new lithology technique. Log Analyst 17 (6), 16–24, SPWLA-1976-vXVIIn6a2.

**Equeenuddin, S.M., Tripathy, S., Sahoo P.K., Ranjan, A.,** 2016. Geochemical characteristics and mode of occurrence of trace elements in coal at West Bokaro coalfield. Int. J. Coal Sci. Technol. 3, 399–406, doi: 10.1007/s40789-016-0146-x

**Fisher, A.T., Underwood, M.B.,** 1995. Calibration of an X-ray diffraction method to determine relative mineral abundances in bulk powders using matrix singular value decomposition: A test from the Barbados accretionary complex, in: Shipley, T.H., Ogawa, Y., Blum, P., et al. (Eds.), Proceedings of the Ocean Drilling Program, Initial Reports. Texas A&M Univ., College Station, Tex., Vol. 156, pp. 29–37, doi: 10.2973/odp.proc.ir.156.103.1995.

**Gandhi, M.S., Solai, A., Chandrasekar, N.,** 2010. Light minerals, XRD and SEM studies in the depositional environments between Tuticorin and Thiruchendur, South East coast of India, Tamil Nadu. Int. J. Geomatic Geosci. 1 (2), 233–251.

**Gholami, R., Rasouli, V., Sarmadivaleh, M., Minaeian, V., Fakhari, N.,** 2016. Brittleness of gas shale reservoirs: A case study from the north Perth basin, Australia. J. Nat. Gas Sci. Eng. 33, 1244–1259, doi: 10.1016/j.jngse.2016.03.013.

**Hillier, S.,** 2003. Quantitative analysis of clay and other minerals in sandstones by X-ray powder diffraction (XRPD), in: Worden, R.H., Morad, S. (Eds.), Clay Mineral Cements in Sandstones. International Association of Sedimentologists, Blackwell, Oxford, pp. 213–251, doi: 10.1002/9781444304336.ch11.

**Jarvie, D.M., Hill, R.J., Ruble, T.E., Pollastro, R.M.,** 2007. Unconventional shale-gas systems: The Mississippian Barnett Shale of north-central Texas as one model for thermogenic shale-gas assessment. AAPG Bull. 91 (4), 475–499, doi: 10.1306/12190606068.

**Jin, X., Shah, S.N., Roegiers, J.-C., Zhang, B.,** 2015. An integrated petrophysics and geomechanics approach for fracability evaluation in shale reservoirs. SPE J. 20, 518–526, doi: 10.2118/168589-PA.

**Lai, J., Wang, G., Huang, L., Li, W., Ran, Y., Wang, D., Zhou, Z., Chen, J.,** 2015. Brittleness index estimation in a tight shaly sandstone reservoir using well logs. J. Nat. Gas Sci. Eng. 27, 1536–1545, doi: 10.1016/j.jngse.2015.10.020.

**Mallick, S.,** 1995. Model-based inversion of amplitude-variations-with-offset data using a genetic algorithm. Geophysics 60 (4), 939–954, doi: 10.1190/1.1443860.

**Singh, S., Qiu, F., Morgan, N., Nath, G., Pritchard, T.,** 2013. Critical comparative assessment of a novel approach for multi-mineral modeling in shale gas: results from an evaluation study of Marcellus Shale, in: SPE Unconventional Resources Conference and Exhibition-Asia Pacific, Brisbane, Australia (11–13 November 2013), SPE-167037-MS, doi: 10.2118/167037-MS.

**Wang, D., Ge, H., Wang, X., Wang, J., Meng, F., Suo, Y., Han, P.,** 2015. A novel experimental approach for fracability evaluation in tight-gas reservoirs. J. Nat. Gas Sci. Eng. 23, 239–249, doi: 10.1016/j.jngse.2015.01.039.

**Wang, F.P., Gale, J.F.W.,** 2009. Screening criteria for shale-gas systems. Gulf Coast Assoc. Geol. Soc. Trans. 59, 779–794.

**Zhang, D., Ranjith, P.G., Perera, M.S.,** 2016. The brittleness indices used in rock mechanics and their application in shale hydraulic fracturing: A review. J. Pet. Sci. Eng. 143, 158–170, doi: 10.1016/j.petrol.2016.02.011.